Journal of Chromatography, 519 (1990) 1–29
Elsevier Science Publishers B.V., Amsterdam

CHROM. 22 670

Flow-through particles for the high-performance liquid chromatographic separation of biomolecules: perfusion chromatography

N. B. AFEYAN*, N. F. GORDON, I. MAZSAROFF, L. VARADY and S. P. FULTON
PerSeptive Biosystems Inc., 38 Sidney St., Cambridge, MA 02139 (U.S.A.)
and
Y. B. YANG and F. E. REGNIER
Department of Biochemistry, Purdue University, Lafayette, IN 47907 (U.S.A.)
(First received January 24th, 1990; revised manuscript received July 2nd, 1990)

ABSTRACT

This paper reports a new technique for reducing resistance to stagnant mobile phase mass transfer without sacrificing high adsorbent capacity or necessitating extremely high pressure operation. The technique involves the flow of liquid *through* a porous chromatographic particle, and has thus been termed "perfusion chromatography". This is accomplished with 6000–8000 Å pores which transect the particle. Data from electron microscopy, column efficiency, frontal analysis and theoretical modelling all suggest that mobile phase will flow through these large pores. In this manner, solutes enter the interior of the particles through a combination of convective and diffusional transport, with convection dominating for Peclet numbers greater than one. The implications of flow through particles on bandspreading, resolution and dynamic loading capacity are examined. It is shown that the rate of solute transport is strongly coupled to mobile phase velocity such that bandspreading, resolution of proteins and dynamic loading capacity are unaffected by increases in mobile phase velocity up to several thousand centimeters per hour.

The surface area of this very large-pore diameter material is enhanced by using a network of smaller, 500–1500 Å interconnecting pores between the throughpores. Scanning electron micrographs show that the pore network is continuous and that no point in the matrix is more than 5000–10 000 Å from a throughpore. As a consequence, diffusional path lengths are minimized and the large porous particles take on the transport characteristics of much smaller particles but with a fraction of the pressure drop. Capacity and resolution studies show that these materials bind and separate an amount of protein equivalent to that of conventional high-performance liquid chromatography as well as low performance agarose-based media at greater than 10–100 times higher mobile phase velocity with no loss in resolution.

INTRODUCTION

Broad application of liquid chromatography to the separation of biological macromolecules began in the late 1950s with the introduction of polysaccharide-based ion-exchange [1] and size-exclusion chromatography [2] columns. Through the use of cellulose, dextrans, and agarose it was possible to prepare supports that were neutral and hydrophilic, easy to derivatize, and sufficiently porous to allow intraparticle transport of macromolecules ranging in size up to more than 500 000 dalton. The great advantage of these supports was that they did not significantly alter the delicate three-dimensional structure of biological macromolecules and they were inexpensive.

0021-9673/90/$03.50

Polysaccharide-based packing materials dominated the chromatography of proteins for more than two decades.

The principal limitation of early polysaccharide supports was their poor mechanical strength; deformation of sorbent particles at pressure differentials of an atmosphere or less was common. Recent commercial efforts to strengthen these materials by extensive crosslinking have increased mechanical stability to the extent that some agarose-based columns will tolerate pressure differentials of 10–20 atm. However, this increase in mechanical strength was achieved at the expense of decreased porosity and increased hydrophobic character of the matrix.

A new era in the liquid chromatography of proteins began in 1976 with the introduction of high-performance liquid chromatography (HPLC) materials based on silica [3]. Because these materials were pressure stable to more than 300 atmospheres, available in particle sizes down to 5 μm, and coated with a hydrophilic phase that gave them the surface properties of soft gels, separations of biological macromolecules could be achieved an order of magnitude faster than on the older soft gel columns with no loss in resolution or biological activity. HPLC revolutionized protein chemistry and had a major impact on the discovery of many new polypeptides. To an extent, the rapid growth and development of biotechnology was heavily dependent on HPLC. An important subset of protein HPLC is fast protein liquid chromatography (FPLC™), which is based on high-performance polymeric supports (Monobeads™) introduced in the early 1980s [4].

Used in an analytical mode, HPLC had a profound impact on modern biochemistry and biotechnology. However, it was not designed to be a preparative technique, and as a consequence almost no attention has been focused on developing sorbents that optimize loading capacity and throughput. Preparative HPLC separations are generally carried out with analytical sorbents in a large version of an analytical column. Second, there is a misunderstanding of how HPLC relates to the chromatographic purification of proteins on polysaccharide-based columns. Because the particles are smaller, stronger, and composed of a different material in HPLC, it is often viewed as a new form of chromatography. It is not! The same fundamental limitations determine resolution in HPLC columns that are at work in soft gel columns. The epoch of using ever decreasing particle size to increase the speed and resolution of liquid chromatography columns, as was done in HPLC, is probably coming to an end. Problems associated with the use of particles smaller than 2 μm in diameter appear to mount exponentially with reduction in particle size. Furthermore, pressure drop and packing considerations limit this technique to analytical uses. Other solutions to increasing the speed and throughput of liquid chromatography columns must be explored.

Separation scientists have been preoccupied for more than four decades with factors that limit the resolution of chromatographic systems. Other than thermodynamic variables controlling distribution coefficients, it is currently accepted that transport efficiency between the stationary and mobile phases is the most dominant variable controlling resolution in liquid chromatography [5]. Reduction of resistance to mass transfer through the use of small particles was a major reason for the success of HPLC.

Solute transport through a chromatographic column occurs predominantly by two mechanisms: (i) convective transport in the mobile phase as it flows between

particles in the column and (ii) diffusive transport through stagnant pools of liquid in the column packing. Obviously, diffusion also occurs within the flowing mobile phase but the ratio of diffusive to convective transport is so small that it is deemed insignificant. Chromatographic separations are generally achieved by differential adsorption of solutes at the surface of packing materials. Thus, solute transport to the sorbent surface is an essential prerequisite in surface mediated separations. Adsorption at the surface of a porous chromatographic packing requires that the solute first diffuse across an immobile film of liquid at the outer surface of the sorbent and then through stagnant pools of liquid in the sorbent pore matrix [5]. The rate at which solute transport processes occur determine both the speed at which a column may be operated and the extent of bandspreading.

"Stagnant mobile phase mass transfer" has been identified as one of the major contributors to peak dispersion in liquid chromatography [5–8]. More than four decades ago Martin and Synge [9] noted in their pioneering work on column chromatography of amino acids that the diffusion of molecules into and out of pores of a packing material would be a major cause of bandspreading and that this phenomenon would be most serious in the case of macromolecules such as proteins. Although advances in the preparation and packing of microparticulate sorbents have diminished the problem of stagnant mobile phase mass transfer [10,11], it is still a serious performance limitation.

It has been shown recently that one extreme solution to this mass transport problem is the elimination of pores entirely [12–14]. Analytical separations have been achieved in less than 60 s with 2–3-μm non-porous particles at mobile phase velocities of 3–5 mm/s. This is possible because resistance to diffusive transport has been minimized. While applicable to analytical separations, unfortunately, this is not a realistic option in preparative chromatography. In addition to rapid transport, high loading capacity must be maintained for high throughput preparative separations. Convective chromatographic packings, wherein diffusion pores are eliminated, suffer from having low surface areas and therefore low binding capacities (typically 1/10 to 1/20 that of porous beads). In effect, columns packed with non-porous particles or microporous membranes represent solutions to the problem of transport kinetics at the expense of surface area. The loss in surface area can be reversed at the expense of increased pressure drop by using ultra-small particles (<1 μm), or membranes with very small diameter pores. This solution is equally impractical, especially for preparative applications considering the low speed dictated by pressure drop, fouling and packing difficulties.

This paper will examine an alternative approach to the problem of intraparticle solute transport in which a combination of convective and diffusive transport modes is used to effect rapid solute transport into porous chromatographic sorbents. Materials that allow such a hybrid mode of transport have been made by engineering not only the porosity but also the permeability of packing materials in order to allow controlled liquid flow through as well as around individual particles. The ramifications of this technology for both analytical and preparative chromatography of biomolecules is described in this paper.

The desirability of enhancing mass transport without the usual penalty of increased pressure drop (momentum transfer) has been suggested by many previous researchers, notably Gibbs and Lightfoot [15]. The literature contains some previous

references to the possible occurrence and adverse implications of flow-through pores in chromatographic supports [16–18]. This prior art was restricted to gel permeation chromatography where it was shown that intraparticle convection would disturb the diffusional process necessary for separation based on size. The only experimental evidence of this is contained within the paper of Van Kreveld and Van den Hoed [17]. They observed that for a large molecule (160 000 mol.wt. polystyrene standard), theoretical plate height became independent of linear velocity at linear velocities above 1 cm/s (3600 cm/h) [17]. They attributed this experimental result to a convective enhancement to stagnant phase intraparticle transport and suggested that this convective enhancement could be "attributed either to eddies or to flow through all or part of the pores". In the absence of information on pore sizes and morphology, it is difficult to differentiate between the postulated mechanisms. The implications of intraparticle convection for adsorptive chromatographic separations were neither realized nor discussed.

THEORY

Numerous reports during the past three decades describe techniques for the fabrication of polymeric particles and membranes for filtration and as catalyst supports that have pores ranging in diameter from 1000 Å to greater than 10 000 Å [19–21]. An attractive feature of these materials is that even a small pressure differential across a membrane with, for instance, 0.5 μm (5000 Å) nominal pore diameter triggers convective flow. It is reasonable to expect that the same phenomenon would occur in beds of sufficiently small particles having interconnected macropores in excess of 5000 Å, where in addition to the normal interstitial flow of mobile phase, liquid would flow through particles. In this case, the extent of throughflow should be governed by the ratio of pore size to particle size. The advantage of this intraparticle convective flow is that it would reduce the time required for intraparticle solute transport and make it possible to speed up the chromatographic process.

Macroporous materials of uniform pore diameter generally have low specific surface area [22]. Thus, a preparative chromatography column filled with uniformly 5000 Å pore diameter sorbent would be of low capacity. It is proposed that this capacity reduction could be reversed by introducing a network of smaller, diffusively fed pores that branch out from the throughpores (Fig. 1). Although this approach again introduces diffusive transport and the problem of stagnant mobile phase mass transfer, the diffusive pores would be very shallow. Convective flow through the arterial channels traversing the particles would cause them to behave as smaller particles in terms of solute transport. Thus, the net effect of introducing large arterial throughpores into a chromatographic packing would be to effectively divide a particle into an aggregate of smaller particles.

Solute transport as described above is similar to the perfusion process in kidneys and other organs. For this reason, the mode of mobile phase transport through this unique chromatographic matrix is referred to as "perfusion" and the separation process itself as "perfusion chromatography" [23]. More specifically, the perfusion threshold is reached when the rate of solute transport by convective flow inside the particles is greater than the rate of diffusive transport driven by concentration gradients. The threshold, in turn, defines a regime wherein perfusion controls solute

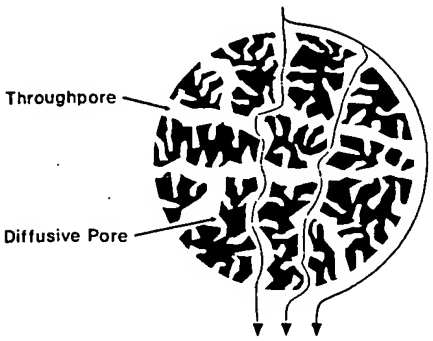

Fig. 1. Diagram of pore structure in a perfusive particle.

transport in the porous network. A "perfusable" particle in this context refers to a porous particle which has interconnected throughpores and which can be operated in the perfusion mode.

Momentum transport

Quantitation of liquid flow through a column relative to flow through particles can be obtained by treating both as packed beds of particles. The Blake–Kozeny correlation [24] can be used to relate the permeability (K) of a packed column to its void fraction (ε_b) as:

$$K = \frac{\varepsilon_b^3}{150(1 - \varepsilon_b)^2} \tag{1}$$

where

$$K = \frac{\eta u_{bed}}{d_p^2 \left(\frac{dp}{dx}\right)_c} \tag{2}$$

and where η is the mobile phase viscosity, d_p is the particle diameter of the support, $(dp/dx)_c$ is the pressure gradient across the column, u_{bed} is the superficial velocity (F/A_c) of mobile phase in the column, F is the flow-rate in ml/min and A_c is the cross-sectional area of the column.

The driving force for perfusive flow across a particle is the column pressure gradient which imposes a pressure difference $(dp/dx)_c\ d_p$ across each particle. Therefore, flow through a permeable particle can be modelled by using the correlation above. Although the exact flow through particles in a packed column will be influenced by the pressure distribution around a particle which in turn is heavily influenced by neighboring particles, a first approximation can be derived by treating the particle as a loosely packed agglomerate of smaller particles (microspheres). Thus, the flow channels are the interstices formed between microspheres. A further assumption that the column pressure drop is mainly due to the interstitial flow around particles (that is,

the flow-rate through the particle is much smaller than that around) is made. Thus, flow through the particle can be described as:

$$u_{\text{pore}} = \frac{K_p d_m^2 \left(\frac{dp}{dx}\right)_c (1 - \varepsilon_b)}{\eta \varepsilon_p} \tag{3}$$

where u_{pore} is the pore velocity, K_p is the permeability of the particle and d_m is the nominal microsphere diameter. Moreover:

$$K_p = \frac{\varepsilon_p^3}{150(1 - \varepsilon_p)^2} \tag{4}$$

and

$$d_m = r d_{\text{pore}}$$

where d_{pore} is the nominal throughpore diameter, ε_p the particle porosity and r a constant related to the closeness of packing (tortuosity).

Conservative estimates for ε_p, r, and ε_b of a sample perfusable support described below (POROS™) are 0.5, 2 and 0.35, respectively. By combining eqns. 1–4:

$$\frac{u_{\text{pore}}}{u_{\text{bed}}} = \frac{K_p}{K}\left(\frac{d_m}{d_p}\right)^2 \frac{(1 - \varepsilon_b)}{\varepsilon_p} \tag{5}$$

Thus, it may be calculated that the average linear velocity of mobile phase through a 7000-Å throughpore in a 10-μm diameter particle is 5% of the average linear velocity through the column bed. So, at 1000 cm/h superficial fluid velocity, the liquid flow through the particle is at least 50 cm/h, equivalent to the superficial fluid velocity of many applications involving soft-gel agaroses.

This analysis may be expanded to account for the ratio of flow through and around particles. It has been approximated that about 2% of the flow traverses through as opposed to around a given particle (data not shown). Thus, the assumption that pressure drop is mainly unaffected by particle throughflow is permissible.

Mass transport

From the preceding discussion, it was shown that for a packed column of perfusable particles, the liquid velocity in the throughpores (u_{pore}) is proportional to the superficial fluid velocity (u_{bed}). Thus for a given column packed with perfusable particles:

$$u_{\text{pore}} = \kappa u_{\text{bed}} \tag{6}$$

Deen [25] has recently reviewed the theoretical framework required to fully characterize transport of macromolecules across a pore through which liquid flow occurs. To a first approximation, the transport of solute into perfusable particles can

be analyzed in an analogous fashion. Transport across throughpores takes place through two distinct modes: the first, diffusive transport, is common to both perfusable and conventional non-perfusable porous particles, while the second is convective transport associated with the liquid flow through the pores.

The ratio of diffusive and convective flux is generally defined as the Peclet number (*Pe*):

$$Pe = \frac{u_{\text{pore}} d_p}{2D} \tag{7}$$

where D is the diffusion coefficient of the solute in the pore.

The perfusion regime, described above, can be practically defined in terms of intraparticle Peclet number. Accordingly, perfusion occurs when $Pe \gg 1$. For instance, the Peclet number for a 10-μm particle with 7000-Å pores, operated at a superficial bed velocity of 1000 cm/h, is approximately 57 (assuming a solute pore diffusivity of $3 \cdot 10^{-7}$ cm^2/s).

Current chromatographic theory only considers diffusive transport into the stagnant mobile phase in a porous support. Consequently, transport is related to the effective pore diffusivity (D), pore length and concentration gradient. In order to adapt the existing equations to also address perfusive supports, the effective diffusivity can be modified to include a convective enhancement factor. A similar approach was used by Van Kreveld and Van den Hoed [17] to account for convective enhancement due to eddy diffusion.

$$D_{\text{eff}} = D + \frac{u_{\text{pore}} d_p}{2} \tag{8}$$

The preceding equation is based on the assumption that the concentration terms governing diffusion and convection can be treated as approximately equal. Mechanistically, this is not accurate because diffusion depends on a concentration gradient while convection is related to the average concentration across the channel. However, this assumption is valid at the limit where the maximum driving force for diffusion and convection are considered, that is, where the pore exit concentration is zero. This treatment is analogous to the coupling theories describing band spreading in chromatography put forth by Giddings [5].

A perfusable particle operated at low superficial fluid velocities, such that $Pe < 1$, is expected to have similar mass transfer characteristics to conventional porous supports. This means that $D_{\text{eff}} = D$. However, in the perfusion regime where $Pe \gg 1$:

$$D_{\text{eff}} \approx \frac{u_{\text{pore}} d_p}{2} \tag{9}$$

Bandspreading analysis

Bandspreading in packed columns of porous supports is often expressed by the Van Deemter equation [26]:

$$H = a + \frac{b}{u_{\text{bed}}} + c u_{\text{bed}} \tag{10}$$

where H is the plate height and a, b and c are lumped terms that account for bandspreading due to longitudinal diffusion, eddy diffusion, mobile phase mass transfer, stagnant phase mass transfer and stationary phase mass transfer. A detailed analysis of the relative accuracy of this versus other expressions of bandspreading are outside the scope of this paper and can be found in numerous publications [5–8]. It suffices to note that the simple Van Deemter equation has been found to be theoretically and experimentally sound.

The c term in this equation refers to band spreading caused by slow pore diffusion. This term dominates the overall extent of bandspreading (plate height) under conditions of high superficial fluid velocity relative to solute diffusivity (or high reduced velocity). Accordingly:

$$H \approx c' \frac{d_p^2 u_{bed}}{D_{eff}} \tag{11}$$

For perfusive supports operated in the perfusion regime, following the treatment presented above, the effective diffusivity is a function of the pore velocity. Pore velocity is, in turn, related to superficial fluid velocity. After making the necessary mathematical substitutions into the Van Deemter equation, one can derive a modified expression:

$$H \approx c' \frac{2 d_p^2 u_{bed}}{\kappa d_p u_{bed}} = \text{constant} \tag{12}$$

Therefore, in the perfusion regime, the plate height is expected to be independent of superficial fluid velocity and remain constant with increasing flow-rate. Interestingly, eqn. 12 also suggests that plate height is related to particle diameter to the first power rather than squared.

The plate height equation presented above is only valid in the perfusion regime. As flow-rate is increased further, intraparticle diffusion into the pores defined by the microspheres, will become rate limiting. Consequently, as with strictly diffusive (conventional) supports, the plate height will increase with increasing flow-rate. However, the slope of this increase (c term in Van Deemter equation) will be much lower and proportional to the mean diffusion path between the throughpores, rather than particle diameter. A more generalized form of the Van Deemter equation which is valid for perfusable supports under all operating conditions has been developed and will be published separately.

Frontal analysis

If a solution of fixed solute concentration (C_0) is fed to a packed column, solute uptake can be characterized by the emerging solute front in the column effluent. The initial solute fed to the column is adsorbed at the active surface and the resulting solute concentration in the column effluent is zero. As time goes on and more solute is loaded onto the column, the column approaches saturation, at which point solute begins to emerge in the column effluent. At the point where the column is saturated to its equilibrium capacity, the solute concentration in the effluent reaches that of the feed.

This elution curve is often referred to as the solute breakthrough curve. Solute breakthrough has been characterized as a function of several parameters [27,28], including mobile phase velocity, an overall transfer coefficient, comprised of many resistances (*e.g.* external film diffusion, internal pore diffusion, adsorption kinetics), equilibrium adsorption parameters, and column and particle geometry.

$$C = \mathrm{f}(M, K_L, Q_{max}, C_0, t, \text{geometry}) \tag{13}$$

where M is an overall mass transfer coefficient, K_L is the equilibrium adsorption constant, Q_{max} is the adsorbent's saturation capacity, C_0 is the solute concentration in the column feed and t is time. With non-perfusive porous supports, as the column flow-rate is increased, capture efficiency decreases and solute emerges prematurely from the column. This behavior becomes more pronounced with increasing flow-rate and effective column loading capacity (dynamic capacity) decreases significantly [29,30].

It has been demonstrated that for most protein/adsorbent systems involving porous particulate supports, the controlling transfer resistance (*i.e.* the slowest step in the process) is internal pore diffusion [28,31–34]. Hence, the overall transfer coefficient, M, can be approximated as follows [28]:

$$M \approx M_{pore} = \frac{60\, D_{eff}(1 - \varepsilon_b)L}{d_p^2 u_{bed}} \tag{14}$$

In the perfusion regime, the effective diffusivity (D_{eff}) is approximated by eqn. 9. Consequently, as in the case of bandspreading (plate height H), the overall mass transfer coefficient, M, is expected to become independent of superficial fluid velocity.

$$M = \frac{30(1 - \varepsilon_b)L\kappa}{d_p} = \text{constant} \tag{15}$$

As a result, with perfusable supports the shape of the breakthrough curve is expected to remain constant as linear superficial fluid velocity increases, and dynamic capacity should remain constant over a wide range of flow-rates.

MATERIALS AND METHODS

Electron microscopy

A Philips EM 420 transmission electron microscope (Philips Electronic Instruments, Mahwah, NJ, U.S.A.) was used for transmission electron microscopy (TEM). Particles of packing material were dispersed on a carbon-coated Formvar film copper grid. The microscope was operated at 80 and 100 kV.

A JEOL JSM-840 scanning electron microscope was used for scanning electron microscopy (SEM). Sorbent particles were applied to double sided adhesive tape (3M Co., St. Paul, MN, U.S.A.) and subsequently affixed to the specimen support. The particles were then sputter coated with platinum and palladium. SEM measurements were made at either 7 or 10 kV as indicated in Figs. 2 and 3.

Chromatography

Supports. POROS™ Q (strong anion-exchange), S (strong cation-exchange) and R (reversed-phase) column packing materials are products of PerSeptive Biosystems (Cambridge, MA, U.S.A.). They have been produced through suspension polymerization techniques and classified to the desired particle size range (nominal diameters are 10 μm for H series and 20 μm for M series). Small columns are flow-packed at 180 bar using a Shandon (Cheshire, U.K.) packer. The 2.54-cm diameter columns were packed at 140 bar using a pump from IBF Biotechnics (Columbia, MD, U.S.A.).

All POROS columns were tested for bandspreading using adenosine monophosphate (AMP) (for Q and S) and phenol (for R) as probe solutes. The reduced plate heights of both small and large columns range between 2–3 for reversed-phase and approximately 4 for ion-exchange, with asymmetry factors below 1.5.

Some experiments were performed with 300- and 1000-Å poly(styrene–divinylbenzene (PS–DVB) particles provided by Polymer Labs. (Shropshire, U.K.). Additional experiments with Mono Q columns (Pharmacia), having nominally 600 Å pores (mean pore size estimated from SEM studies performed by authors; no actual measurements reported by vendor), were also performed.

Equipment. Several liquid chromatographic systems were used for the experiments reported in this study; they are: (a) Hewlett-Packard HP 1090 (Waldbronn,

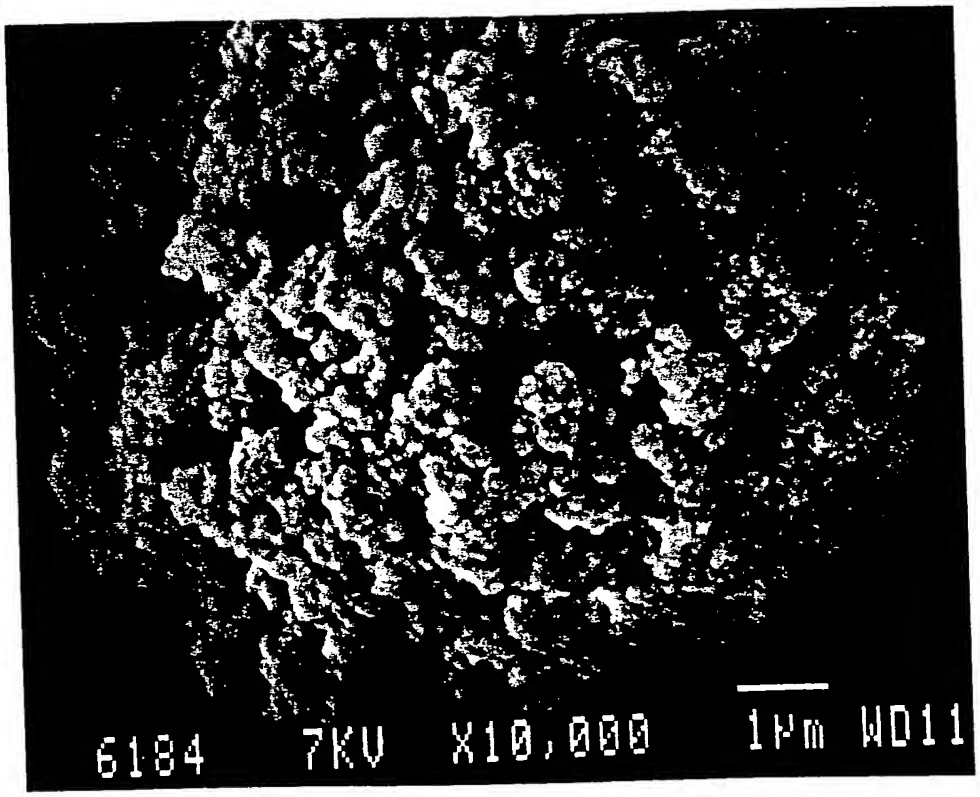

Fig. 2. Scanning electron micrograph of POROS R/H.

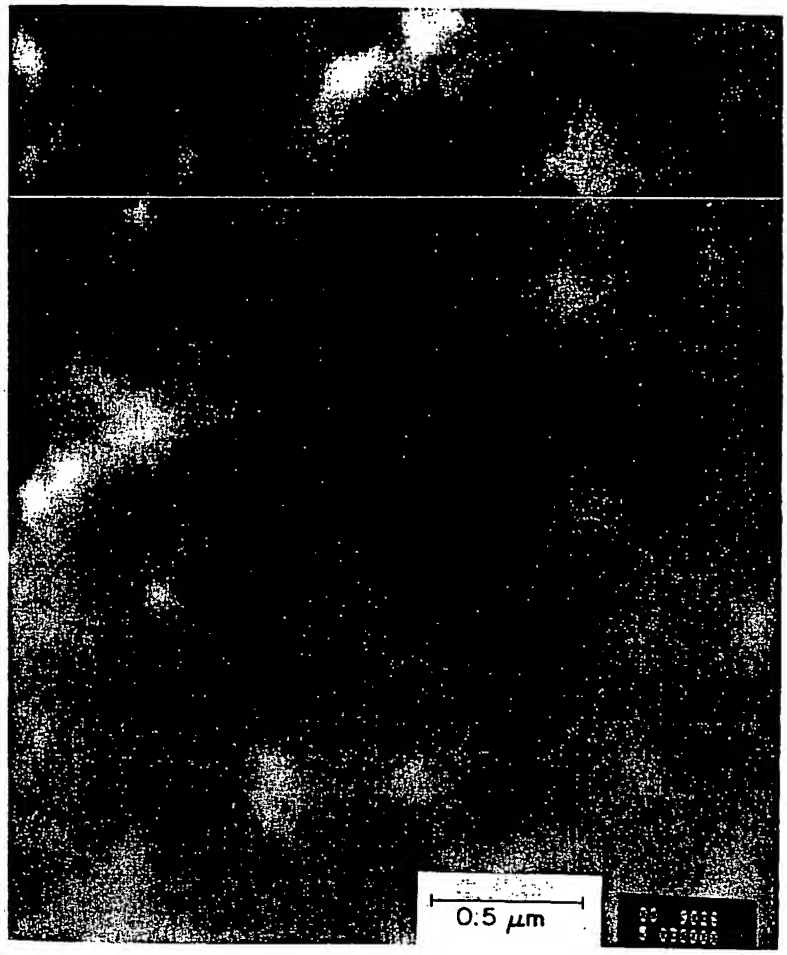

Fig. 3. Transmission electron micrograph of POROS R/H.

F.R.G.) equipped with a diode array detector, automatic injector, column switching valve and a "Chem Station" for data acquisition and system control. (b) Hewlett-Packard HP 1050 equipped with a variable-wavelength detector, Rheodyne injection valve and a Hewlett-Packard integrator. (c) Waters Delta-Prep (Milford, MA, U.S.A.), fitted with 180 ml/min pump heads, variable-wavelength detector, sample loader, and a computer system (PC AT) operating Dynamic Solutions software. (d) IBF Biotechnics pump with flow-rate capacity up to 1 l/min.

Materials. All standard proteins were obtained in purified form from Sigma (St. Louis, MO, U.S.A.) except where noted otherwise. All solvents were HPLC grade where appropriate. Hybridoma cell culture supernatant was obtained from perfusion culture with a defined medium. The predominant contaminant is albumin. *E. coli* extract was obtained from a 1000-l fermentation [35]. The fermentation broth was concentrated, the cells were disrupted, cell debris removed, followed by an ammonium sulphate precipitation. The pellet was resuspended in piperazine buffer (pH 6).

Calculation of column efficiency

Column efficiency (*e.g.* plate height) was estimated using a non-retained solute. For the purposes of this analysis, conditions of non-retention were determined as roughly twice that required to cause elution in the gradient mode. The test solute was dissolved in the mobile phase, and a sample was injected onto an equilibrated column. The resulting chromatogram was recorded and the reduced plate height, h, calculated as follows:

$$N = 5.54\left(\frac{V_t}{W}\right)^2$$

and

$$h = \frac{L}{Nd_p}$$

Resolution was calculated according to the method described by Snyder and Kirkland [8]. Frontal chromatography results have been normalized to the volume at which solute begins to emerge in the column effluent.

RESULTS AND DISCUSSION

The premise that mobile phase will flow through highly porous particles under a relatively small pressure differential is pivotal in the theory of perfusion chromatography. Unfortunately, experimental confirmation of this hypothesis is difficult. Experimental techniques that test liquid flow through a 10-μm porous particle have not been described. As a consequence, an indirect method must be used. The easiest approach, and the one chosen for these studies, is to compare the properties of candidate systems to what the theory would predict for a packed bed of perfusable particles. Because the properties of perfusable materials should be dramatically different from conventional chromatographic sorbents, convective flow through particles will be confirmed by inference. Four techniques were used to examine candidate perfusion materials; (1) electron microscopy, (2) plate height analysis, (3) frontal analysis characteristics and (4) rapid separations of protein and peptide mixtures at high mobile phase velocity.

Chromatographic sorbents

The POROS family of chromatographic packings was used for all experiments reported in this paper except where noted to the contrary. These PS–DVB-based materials are the result of an endeavor to fabricate matrices with the properties shown in Fig. 1. These particles have a void fraction (ε_p) of approximately 0.5 and pack into a bed with an interstitial volume (ε_b) of about 35% of the column volume. Columns (100 × 4.6 mm I.D.), packed with POROS, were found to be mechanically stable to a pressure differential of 250 bar (3750 p.s.i.) with both the series H (10 μm) and M (20 μm) packings. Moderate overpressuring did not seem to harm the packing. An SEM study of series H reversed-phase sorbent, which had been overpressured at 400 bar

(6000 p.s.i.), showed that the packing was neither permanently deformed nor broken (data not shown).

Electron microscopy

A scanning electron micrograph of POROS R/H is shown in Fig. 2. The micrograph reveals that the particle is an agglomerate of microspheres that are fused into a continuous structure. The manner in which the aggregates are fused creates the pore matrix. Because these agglomerates are not tightly packed, several types of pores are present in the matrix. The largest of these pores are approximately 6000–8000 Å in diameter, and are equivalent to the throughpores shown in Fig. 1. A second, more abundant set of pores are of 500–1500 Å in diameter. These pores are generally interconnected but are thought to be too small to allow appreciable liquid flow, and are thus, accessed primarily by diffusion. It is significant that these pores are seldom more than 1 μm deep. The smallest pores in the particle are shallow cavities or psuedopores that result from the rough texture of the pore matrix. These cavities are never more than a few hundred angstroms deep but are seen, in the SEM, to contribute substantially to the surface area of the sorbent.

An essential component of the theory of perfusion is that a significant number of large pores transect the particle, providing the through-flow channels for rapid solute access to the high surface area regions of the particle. The presence of large pores on the surface of the particle, alone, does not prove that they transect the particle. A transmission electron micrograph of a POROS R/H particle (Fig. 3) provides strong evidence of throughpores. The electron beam is seen to pass through the particle at specific sites. The interpretation of this micrograph is that these sites of high exposure are the result of electron diffraction through large pores that transect the support.

Taken together, the electron micrographic data provide a physical picture of the pore matrix that allows the following conclusions to be made. First, there are very large pores that transect the sorbent. Second, these pores are of sufficient size, as experience has shown with membrane systems, that a small pressure differential should trigger convective flow through the particle. Third, there is a network of smaller pores in the matrix that are connected to the large throughpores. Finally, the spacing between throughpores is seldom greater than 1 μm in any plane. This means that solute diffusion distance in the diffusively fed pore matrix would generally be less than 5000–10 000 Å.

Band spreading

Theory suggests that perfusion of mobile phase through a particle will dramatically reduce resistance to stagnant mobile phase mass transfer and increase column efficiency, particularly at high mobile phase velocity. In the context of inferring convective flow through particles by correlation with another chromatographic parameter, column efficiency (reduced plate height) was examined as a function of mobile phase velocity.

The reduced plate height of insulin (non-retained) in reversed-phase columns is presented as a function of mobile phase velocity for POROS R/H, POROS R/M, and a 300-Å (10 μm) HPLC support in Fig. 4. At the highest mobile phase velocity of 6000 cm/h, solute residence time in a 3-cm column was *ca.* 2 s. Several important features of these plate height curves should be noted. First, it is seen that the POROS matrix is of

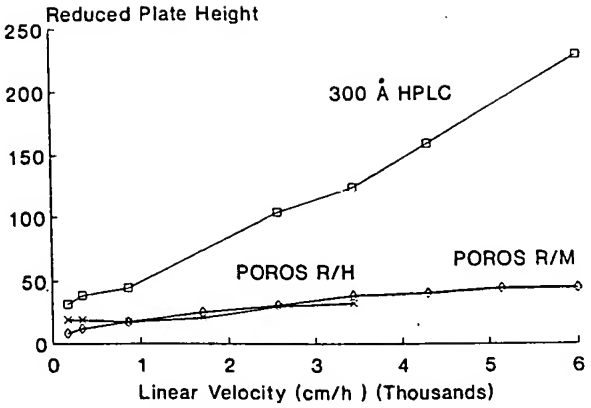

Fig. 4. Column efficiency *versus* flow-rate. Non-retained insulin; acetonitrile–water (50:50); 0.5 μg injection; detection at 214 nm. (a) POROS R/M, 30 × 2.1 mm I.D. column; (b) POROS R/H, 30 × 2.1 mm I.D. column; (c) 300 Å HPLC, 30 × 2.1 mm I.D. column.

much greater efficiency at high mobile phase velocity than the HPLC sorbent. Second, reduced plate height is only weakly related to mobile phase velocity with the POROS sorbents. Third, the reduced plate height of the 10- and 20-μm POROS supports are equivalent, even with increasing flow-rate. Conventional LC theory predicts that the performance of these two particle sizes should differ by a factor equivalent to the ratio of their diameters. It is proposed that the superior efficiency of these sorbents at high mobile phase velocity is due to convective flow through the pore matrix of the particle as predicted in eqn. 13.

Similar differences between the reduced plate height curves of POROS and wide pore HPLC materials were noted in anion-exchange separation of both proteins and mononucleotides. Fig. 5 shows the plate height–flow-rate dependence for non-retained bovine serum albumin in the anion-exchange mode for POROS Q/M and a 1000-Å HPLC support of the same particle size and surface chemistry. Finally Fig. 6 shows similar results for non-retained AMP with the same two supports. It may be concluded from the plate height curves shown above that intraparticle solute transport in the POROS particles is substantially uncoupled from the mobile phase velocity. Therefore, that portion of the loss in resolution that is due to increased bandspreading at high superficial fluid velocities, seen with non-perfusable supports, is expected to be minimized with these particles.

Frontal analysis

Frontal uptake of protein by a chromatographic column provides another method for kinetically differentiating between support materials. When a protein solute is pumped through a column very slowly, residence time in the column is sufficient to overcome mass transfer limitations. Under these conditions, solute emerges from the column in a sharp step after the sorbent has been saturated. The specific binding capacity of the sorbent in this case is identical to the static loading capacity obtained in batch adsorption studies that allow long equilibration times. When protein solutions are pumped through sorbent beds at higher velocities, specific

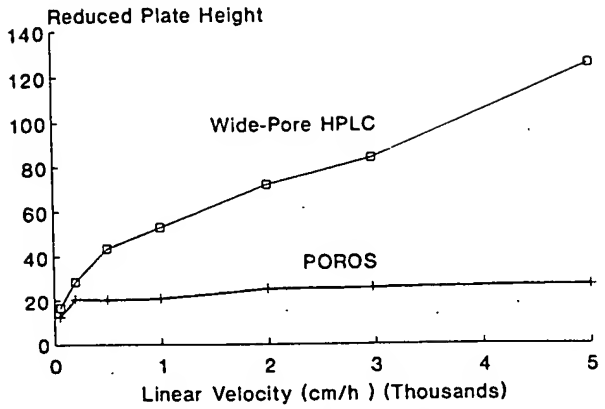

Fig. 5. Column efficiency *versus* flow-rate. Non-retained bovine serum albumin; 20 m*M* Tris–HCl buffer, pH 8 + 0.5 *M* NaCl; 6 μg injection; detection at 280 nm. (a) POROS Q/M, 30 × 2.1 mm I.D. column; (b) 1000 Å HPLC Q, 30 × 2.1 mm I.D. column.

loading capacity generally decreases [25,26]. This kinetically based reduction in loading capacity is quantitatively manifested as a premature emergence of protein in the breakthrough curve. Differences in the static and dynamic loading capacity of a sorbent are a sensitive measure of mass transfer limitations. It has been shown that particle size, sorbent pore size, column geometry and mobile phase velocity all influence dynamic loading capacity and the solute breakthrough curves [25,26]. A typical breakthrough curve on a sorbent that is completely saturated, *i.e.* at equilibrium, is shown in Fig. 7. Dynamic loading capacity is determined from this curve by calculating the amount of protein that has been pumped onto the column when the concentration of protein in the column effluent rises above 5–10% of that in the feed stream.

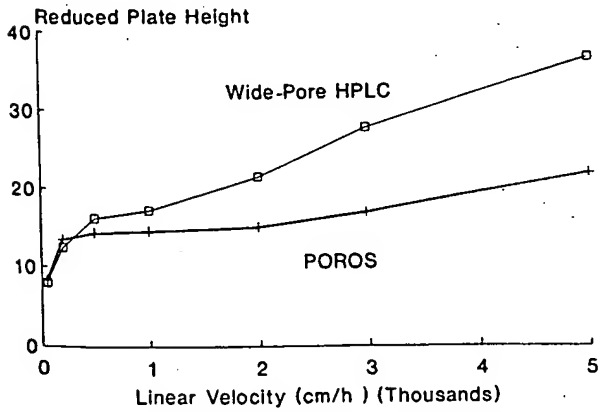

Fig. 6. Column efficiency *versus* flow-rate. Non-retained AMP; 0.1 *M* phosphate buffer, pH 2.6; 0.6 μg injection; detection at 254 nm. (a) POROS Q/M, 30 × 2.1 mm I.D. column; (b) 1000-Å HPLC, 30 × 2.1 mm I.D. column.

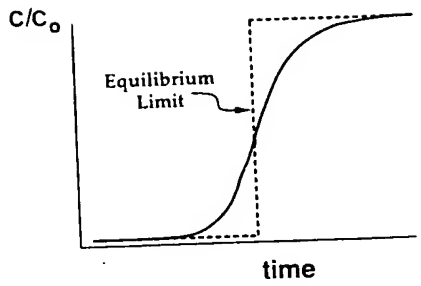

Fig. 7. Generalized solute breakthrough curve.

The influence of mobile phase velocity on the protein loading capacity of a 10-μm, nominal 600 Å pore diameter HPLC support (Mono Q) is shown in Fig. 8. At a linear velocity of 50 cm/h, the dynamic and static loading capacity were similar. This means that at this mobile phase velocity, there was sufficient contact time to allow complete saturation of the column before solute began to emerge. However, as mobile phase velocity was accelerated, premature solute breakthrough was observed. When the linear velocity reached 2500 cm/h, dynamic loading capacity was reduced to 60% of the static capacity due to severe premature solute breakthrough.

Frontal breakthrough curves for POROS Q/M and Q/H are shown in Figs. 9 and 10. The frontal analysis data has been normalized such that the volume at which 50% breakthrough occurs (inflection point) is designated as 100% of breakthrough volume. The broader the breakthrough curve, the greater the volume over which breakthrough

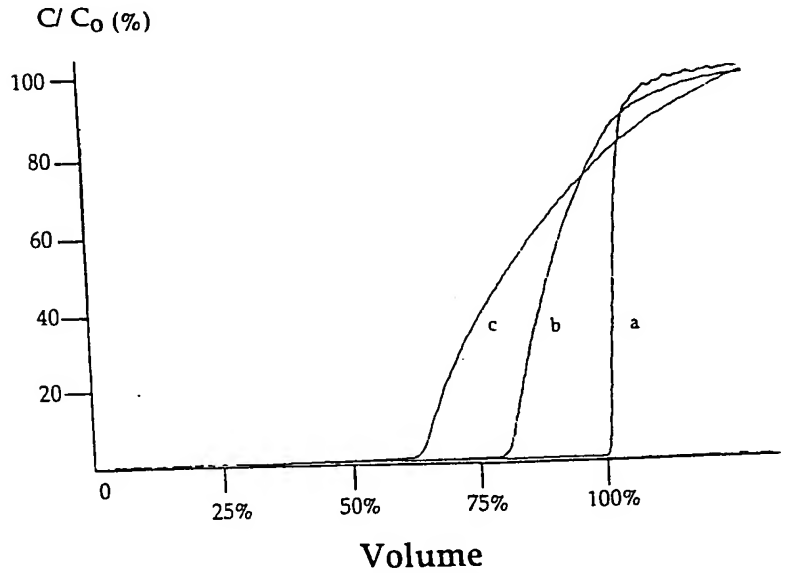

Fig. 8. Solute breakthrough curve for 10-μm particle diameter diffusive support; 2 mg/ml bovine serum albumin dissolved in 20 m*M* Tris–HCl, pH 8.0; 30 × 2.1 mm I.D. column; detection at 280 nm. (a) 0.029 ml/min; 50 cm/h; (b) 0.58 ml/min; 1000 cm/h; (c) 1.44 ml/min; 2500 cm/h.

occurs, and hence, the lower the dynamic loading capacity. The data show that the breakthrough volume increases minimally as superficial bed velocity increases, and thus, dynamic and static loading capacity are equivalent. This result is in direct contrast to the results shown in Fig. 8 (diffusion limited case), where dynamic loading capacity decreased considerably with increasing mobile phase velocity. Based on these data, it may be concluded that the resistance to mass transport, as judged by frontal analysis, is substantially smaller in the very high porosity throughpore materials. It is proposed that this is the result of these highly porous, permeable, materials being operated in a perfusion regime as shown in eqn. 15.

The static bovine serum albumin loading capacity of POROS Q/M under the conditions of Fig. 9 was approximately 75% the capacity of the HPLC support (Fig. 8). However, unlike the latter, the dynamic and static capacity of POROS Q remain equivalent even at flow-rates exceeding 5000 cm/h. Dynamic loading capacity is a more meaningful measure of the utility of a preparative chromatography packing than static capacity because it relates to the capacity of a column under the conditions it is being operated. For example, it has been shown with bovine serum albumin that the loading capacity of 10-μm anion-exchange sorbents of 250 and 500 Å pore diameter are 10 and 40% respectively of the static loading capacity when the columns were operated at 600 cm/h linear velocity [26]. Furthermore, materials with the highest static loading capacity generally had the lowest dynamic loading capacity at this mobile phase velocity.

Fig. 11 compares the dynamic loading capacity of POROS with that of Fast Flow Sepharose. Data for the dynamic loading capacity of Fast Flow Sepharose were taken from the literature [36]. Available data reveal (1) that the loading capacity of POROS is constant up to a linear velocity of 5000 cm/h as theory predicts and (2) that the dynamic loading capacity of POROS is many times greater than that of either HPLC or soft gel sorbents at high mobile phase velocity. Since dynamic loading capacity and the time required to load a column are major contributors to throughput in preparative chromatography, it is seen that any sorbent which can impact these variables by orders of magnitude will be of substantial utility in preparative chromatography.

High-speed separations

Both the plate height curves (Figs. 4–6) and theory predict that intraparticle perfusion would allow extremely high mobile phase velocity and throughput with little loss in either resolution or capacity, at moderate pressure. This prospect was examined with the high porosity POROS matrix alone and in comparison with conventional wide-pore HPLC sorbents. Anion-exchange, cation-exchange and reversed-phase separations in the gradient elution mode are reported below. Gradient slope (in % change/ml) and total elution volumes were the same in all cases where flow-rate and gradient time were varied.

The influence of matrix porosity on resolution at high mobile phase velocity is seen in the analytical anion exchange separations in Figs. 12 and 13. Resolution of ovalbumin (OVA) and soybean trypsin inhibitor (STI) at 1, 2 and 4 ml/min on POROS Q/H was 6.0, 6.5 and 6.2, respectively. It should be noted that the relative difference in conalbumin (CON) concentration in these chromatograms is the result of sample aging. Approximately one week elapsed between the separations carried out at 1 and

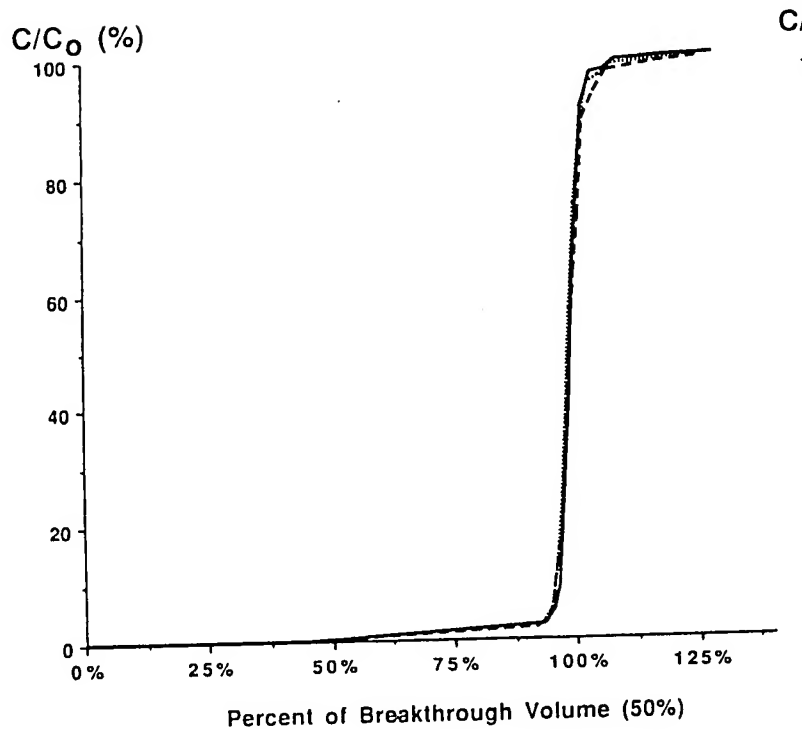

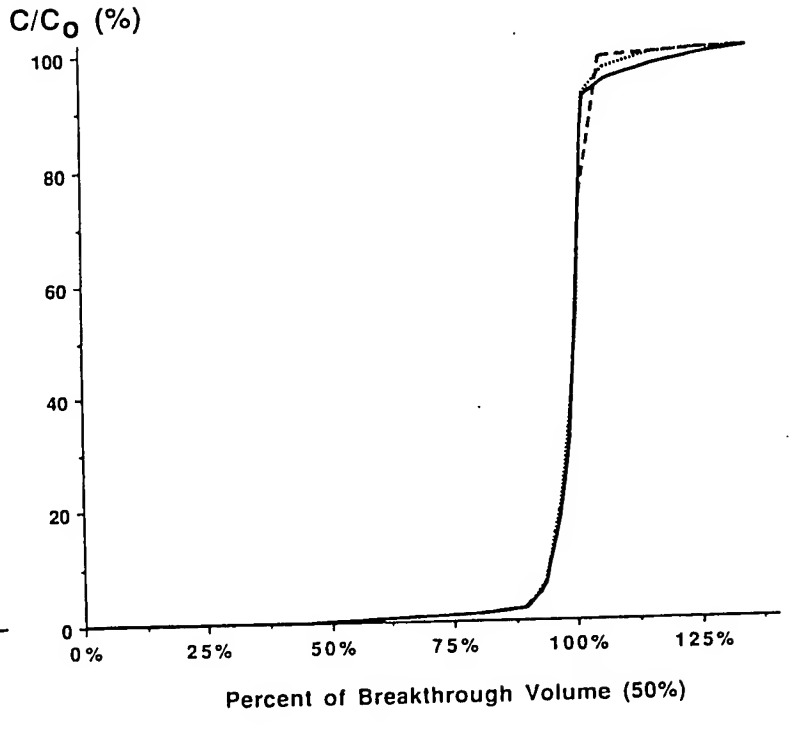

Fig. 9. Solute breakthrough curve for POROS Q/M; 0.1 mg/ml bovine serum albumin dissolved in 20 m*M* Tris–HCl, pH 8.0; 30 × 2.1 mm I.D. column; detection at 280 nm. ——— = 0.58 ml/min, 1000 cm/h; ····· = 1.2 ml/min, 2000 cm/h; --------- = 2.0 ml/min, 3500 cm/h.

Fig. 10. Solute breakthrough curve for POROS Q/H; 0.1 mg/ml bovine serum albumin dissolved in 20 m*M* Tris–HCl, pH 8.0; 30 × 2.1 mm I.D. column; detection at 280 nm. ——— = 0.58 ml/min, 1000 cm/h; ····· = 1.2 ml/min, 2000 cm/h; --------- = 2.0 ml/min, 3500 cm/h.

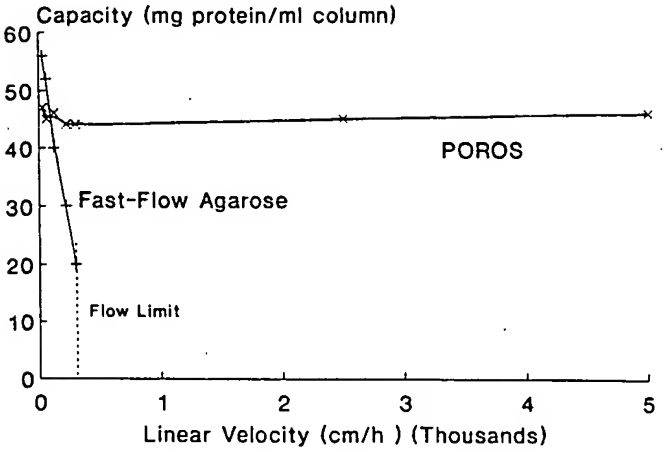

Fig. 11. Dynamic bovine serum albumin capacity *vs.* flow-rate, + = Q-Sepharose Fast Flow; × = POROS Q/M.

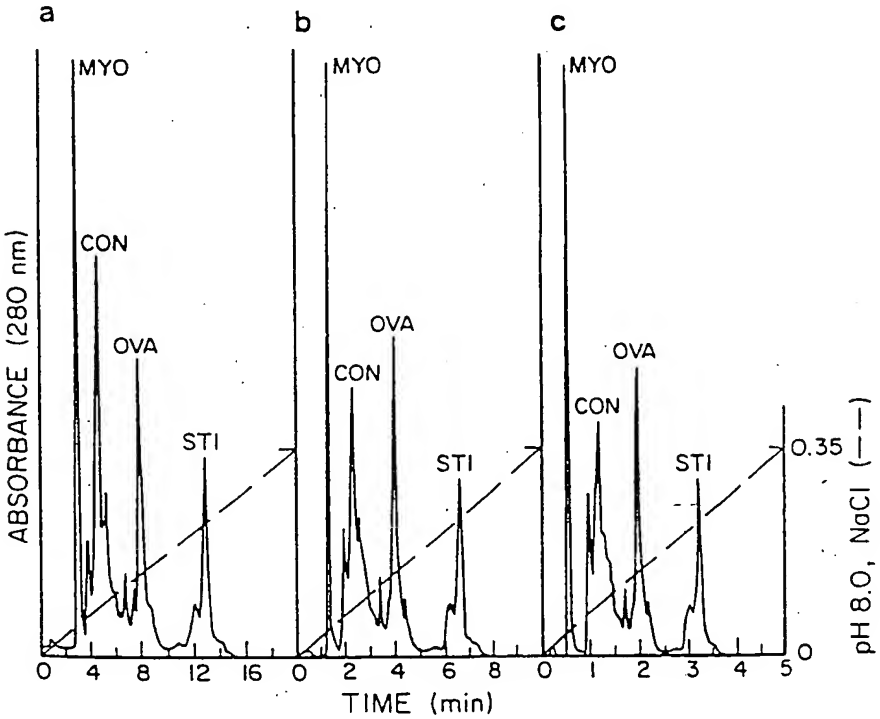

Fig. 12. Separation of model proteins on POROS Q/H; 350 μg load of a protein mixture containing myoglobin, conalbumin, ovalbumin and soybean trypsin inhibitor; detection at 280 nm; column, 50 × 4.6 mm I.D.; 10 m*M* Tris–HCl buffer, pH 8.0. (a) 1 ml/min; 20-min gradient to 0.35 *M* NaCl; (b) 2 ml/min; 10-min gradient to 0.35 *M* NaCl; (c) 4 ml/min; 5-min gradient to 0.35 *M* NaCl.

Fig. 9. Solute breakthrough curve for POROS Q/H; 0.1 mg/ml bovine serum albumin dissolved in 20 m*M* Tris–HCl, pH 8.0; 30 × 2.1 mm I.D. column; detection at 280 nm. ——— = 0.58 ml/min, 1000 cm/h; ····· = 1.2 ml/min, 2000 cm/h; ------ = 2.0 ml/min, 3500 cm/h.

Fig. 10. Solute breakthrough curve for POROS Q/H; 0.1 mg/ml bovine serum albumin dissolved in 20 m*M* Tris–HCl, pH 8.0; 30 × 2.1 mm I.D. column; detection at 280 nm. ——— = 0.58 ml/min, 1000 cm/h; ····· = 1.2 ml/min, 2000 cm/h; ------ = 2.0 ml/min, 3500 cm/h.

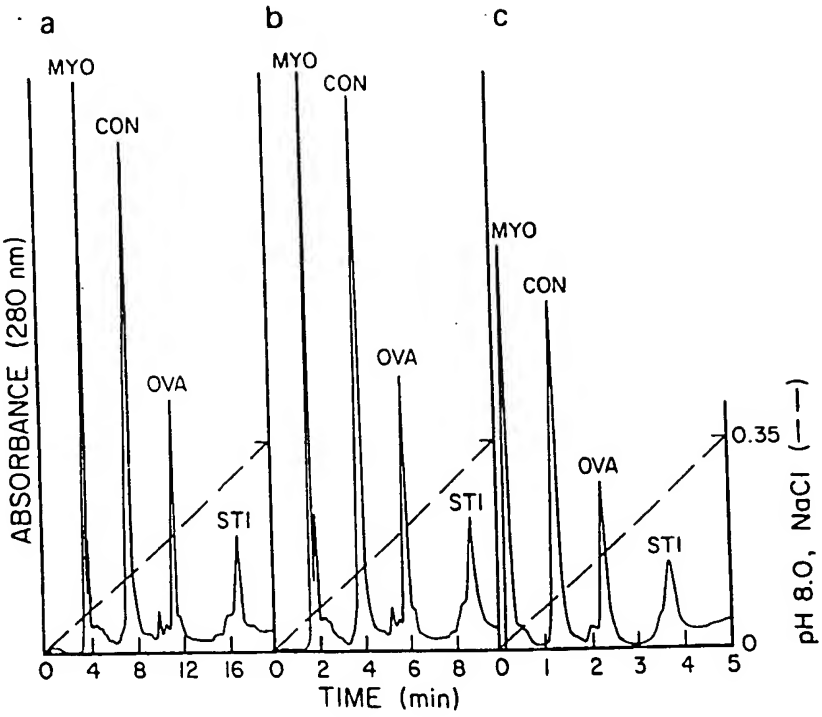

Fig. 13. Separation of model proteins on 1000-Å HPLC support (Q); 350 μg load of a protein mixture containing myoglobin, conalbumin, ovalbumin and soybean trypsin inhibitor; detection at 280 nm; column, 50 × 4.6 mm I.D.; 10 m*M* Tris–HCl buffer, pH 8.0. (a) 1 ml/min, 20-min gradient to 0.35 *M* NaCl; (b) 2 ml/min; 10-min gradient to 0.35 *M* NaCl; (c) 4 ml/min; 5-min gradient to 0.35 *M* NaCl.

4 ml/min. Whereas resolution was independent of mobile phase velocity with the high-porosity sorbent, resolution decreased markedly at high mobile phase velocity on a 1000 Å nominal pore diameter PS–DVB matrix derivatized with the same stationary phase. Resolution of the OVA–STI mixture on the 1000-Å pore diameter material at 1, 2 and 4 ml/min was 6.3, 5.4 and 3.6, respectively. This difference in the resolving power of these two matrices at high mobile phase velocity is attributed to the dominance of convective transport in the high porosity material.

Further examples of the ability to increase mobile phase velocity with minimal loss of resolution when using very-high-porosity, permeable, sorbents are seen in the analytical separations in Figs. 14–17. Figs. 14 and 15 show the separation of a model protein mixture, at increasing superficial fluid velocity, in POROS S and POROS R columns, respectively. Fig. 16 shows the separation of immunoglobulin G from a cell culture supernatant on a POROS Q/M column and Fig. 17 shows the separation of three variants of angiotensin on the POROS R/M column. Because this phenomenon was seen in three different separation modes with a variety of proteins and peptides, it may be concluded that it is neither mode nor compound specific.

Studies on preparative separations produced similar results (Figs. 18 and 19). The behavior of POROS Q/M and a wide-pore HPLC anion-exchange sorbent is quite different in the preparative separation of an ovalbumin–bovine serum albumin

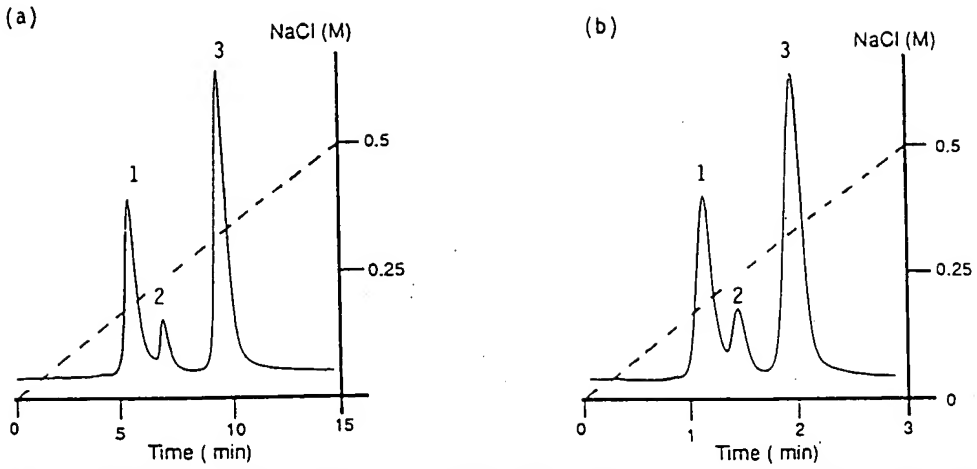

Fig. 14. Separation of model proteins on POROS S/M; 75 μg load of a protein mixture containing chymotrypsin (1), cytochrome *c* (2), and lysozyme (3); detection at 280 nm; column, 100 × 4.6 mm I.D.; 20 m*M* 2-[N-morpholino]ethanesulfonic acid buffer, pH 6.0; detection at 280 nm. (a) 1 ml/min, 15-min gradient to 0.5 *M* NaCl; (b) 5 ml/min; 3-min gradient to 0.5 *M* NaCl.

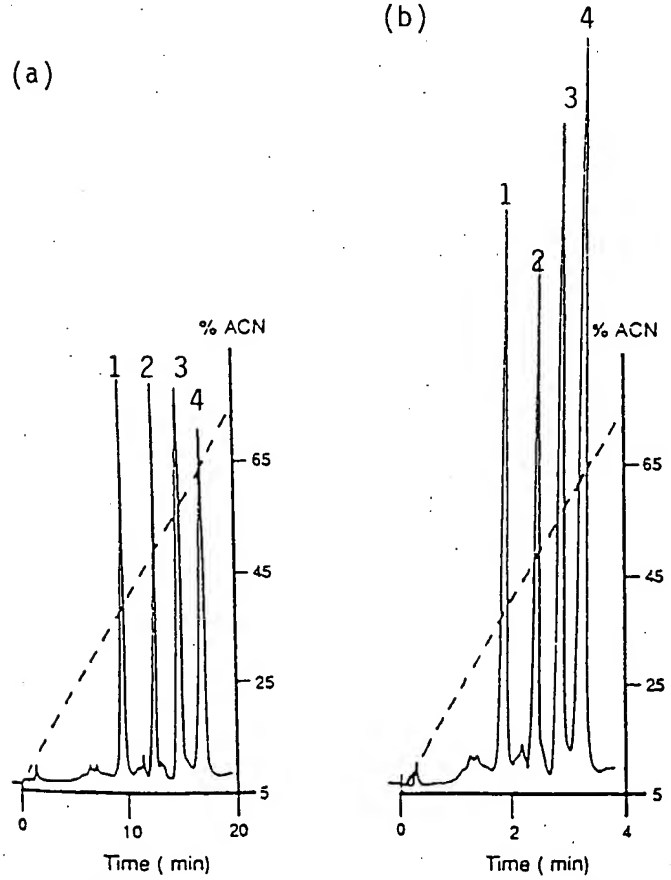

Fig. 15. Separation of model proteins on POROS R/M; 100 μg load of a protein mixture containing ribonuclease A (1), lysozyme (2), β-lactoglobulin (A and B) (3) and ovalbumin (4); detection at 280 nm; column, 100 × 4.6 mm I.D.; 5% acetonitrile (ACN) + 0.1% trifluoroacetic acid in water. (a) 1 ml/min, 20-min gradient to 70% acetonitrile; (b) 5 ml/min; 4-min gradient to 70% acetonitrile.

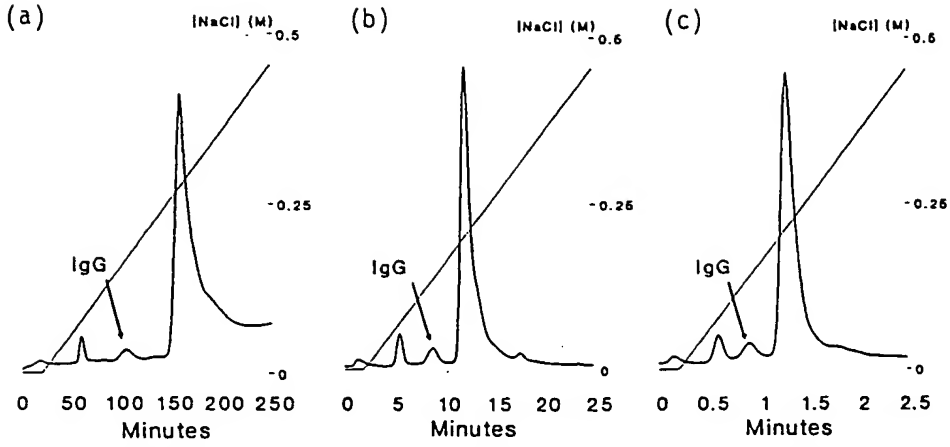

Fig. 16. Separation of immunoglobulin G from hybridoma cell culture supernatant on POROS Q/M; 500 μg load (total protein) of crude cell culture supernatant; column: 100 × 4.6 mm I.D.; 20 m*M* Tris–HCl buffer, pH 8.0; detection at 280 nm. (a) 0.1 ml/min, 250-min gradient to 0.5 *M* NaCl; (b) 1 ml/min; 25-min gradient to 0.5 *M* NaCl; (c) 10 ml/min; 2.5-min gradient to 0.5 *M* NaCl.

mixture (Fig. 18). Resolution of the POROS matrix decreased with sample load but was relatively independent of mobile phase velocity, particularly at high loading. In contrast, preparative resolution on the wide-pore HPLC sorbent was very sensitive to mobile phase velocity. Minimal coupling of mobile phase velocity and resolution was also seen in preparative reversed-phase separation on POROS R/M (Fig. 19).

An example of preparative scale-up is seen in Fig. 20. Separation of β-galactosidase from a clarified *E. coli* homogenate is shown at three different scales of operation, ranging from a 4-mg load on a 1.7-ml column to a 76-mg load on a 51-ml column. Gradient slope was the same in all cases. It may be concluded from these studies that preparative separations can be carried out at high resolution in time frames comparable to very fast analytical systems.

Implications

These very-high-speed preparative separations raise the question of how this technology relates to biotechnology and large-scale production of proteins. It has been the practice for more than two decades to carry out preparative separation of proteins in large, low-efficiency soft gel columns with 1–10-h separation times being the norm. Most of the first generation of "recombinant" proteins are produced with this old technology, the general protocol being to use columns of sufficient size to process all of the product produced in a single run of a fermentor. Much smaller columns of higher productivity can also be used for these tasks. Such columns that process large amounts of protein through multiple separation cycles would function equally well, but offer significant economic advantages. It is in this area of rapid cycling preparative systems that perfusion chromatography can have an enabling impact.

The efficiency of a preparative column may be judged by specific throughput or productivity, *i.e.* mass of product produced/volume of column/unit time. Based on the dynamic capacity data presented in Fig. 11, column productivity was determined as follows. The chromatographic cycle time was calculated as the amount of time

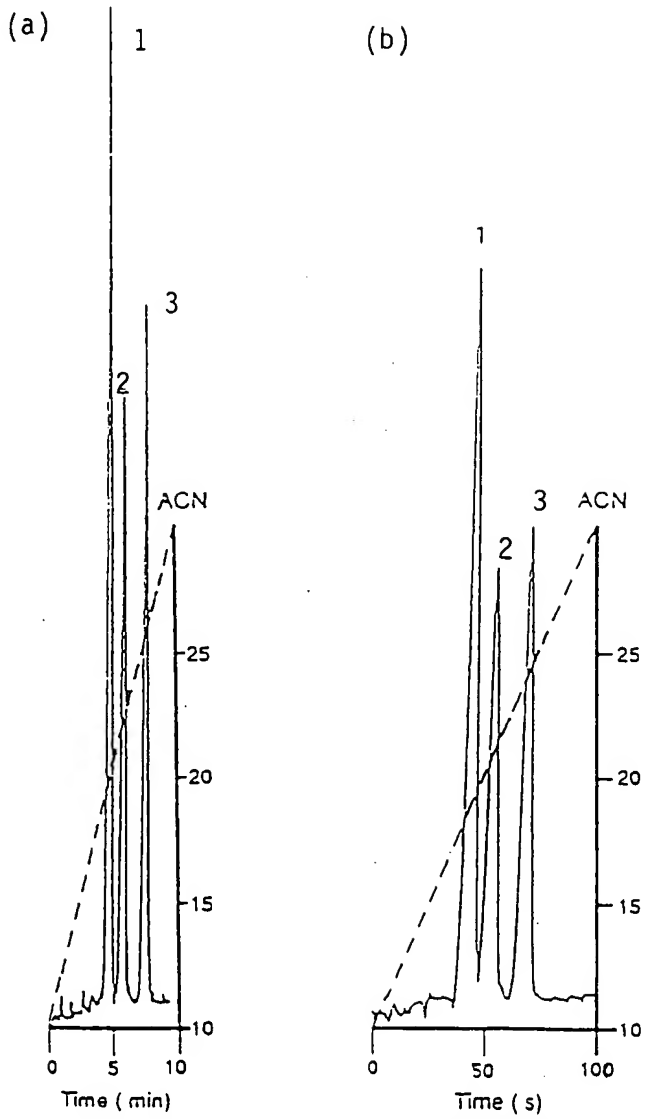

Fig. 17. Separation of angiotensin variants on POROS R/M; 20 μg load each of [Val^4, Ile^7]angiotensin III (1), [Val^4]angiotensin III (2) and angiotensin III (3) dissolved in the mobile phase; column, 100 × 4.6 mm I.D.; 5% acetonitrile (ACN) + 0.1% trifluoroacetic acid in water; detection at 230 nm. (a) 1 ml/min, 9-min gradient to 30% acetonitrile; (b) 5 ml/min; 1.8-min gradient to 30% acetonitrile.

required to load the sample as well as the time required to wash, elute and regenerate the column (estimated to require 15 column volumes). At a given flow-rate, the dynamic loading capacity dictates the amount of feed that can be applied as well as the time for the loading step. Subsequent steps in the chromatographic cycle (wash, elute, regenerate) were assumed to be conducted at the same flow-rate as the initial loading step.

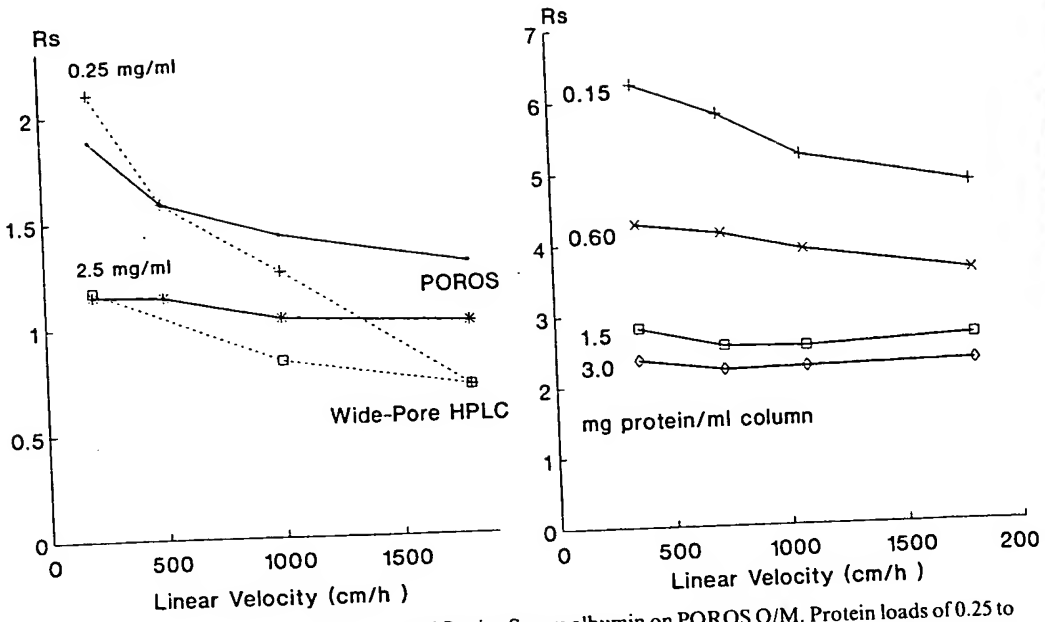

Fig. 18. Resolution (R_s) of ovalbumin and Bovine Serum albumin on POROS Q/M. Protein loads of 0.25 to 2.5 mg protein/ml column were loaded at flow-rates of 0.5, 1, 2, 3, 4 and 5 ml/min; column, 100 × 4.6 mm I.D.; 20 m*M* Tris–HCl buffer, pH 8.0; 25-ml gradient to 0.5 *M* NaCl; detection at 280 nm.

Fig. 19. Resolution of ribonuclease A and lysozyme on POROS R/M. Protein loads ranging from 0.15 to 3.0 mg protein/ml column were loaded at flow-rates of 1, 2, 3, 4 and 5 ml/min; column, 100 × 4.6 mm I.D.; 4% acetonitrile + 0.1% trifluoroacetic acid in water; 20 ml gradient to 70% acetonitrile; detection at 280 nm.

The specific throughput of Fast Flow Sepharose and POROS as a function of mobile phase velocity is shown in Fig. 21. It is seen that the soft gels inherently operate at a low productivity. Due to mass transfer limitations, increasing the mobile phase velocity beyond 300 cm/h becomes counter productive. In addition, mechanical strength limitations of this support, can further limit the operating range to less than 100 cm/h, depending on the column length employed. However, the specific throughput in the case of POROS, increases with linear velocity, even up to 4000 cm/h. The superior specific throughput of this material is again attributed to intraparticle convective transport.

Breakthrough analysis, in addition to being a powerful measure of kinetic resistances to binding, has direct relevance to bioprocessing. An important application of column chromatography is the capture and concentration of a product from a dilute bioreactor effluent. This process is usually performed using agarose-based fast-flow supports in one of the adsorptive modes (ion-exchange, affinity, hydrophobic-interaction), by typically operating the columns at $\leqslant 100$ cm/h. Higher velocities result in greatly reduced bed capacities and/or compression of the packed bed. A high throughput alternative to this process would be the use of perfusable sorbents, operated at superficial fluid velocities of 2000–5000 cm/h. Fig. 22 shows that the breakthrough profile of a 50 ml (10 × 2.54 cm) POROS Q/M column operated at 2400

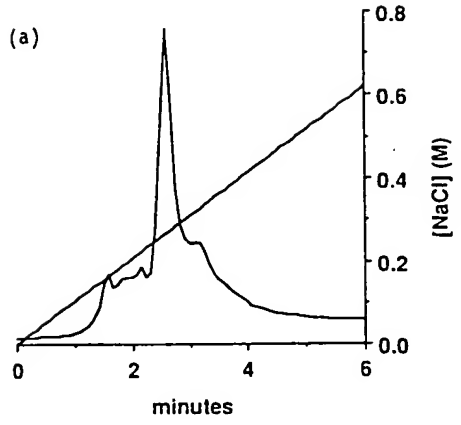

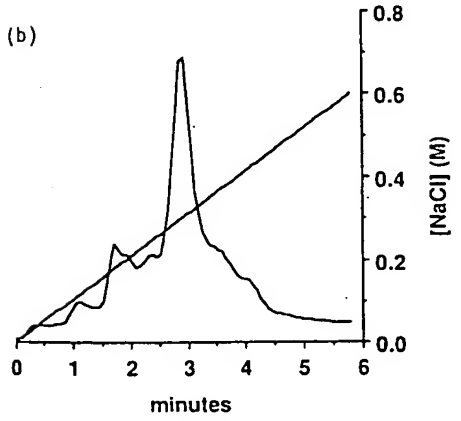

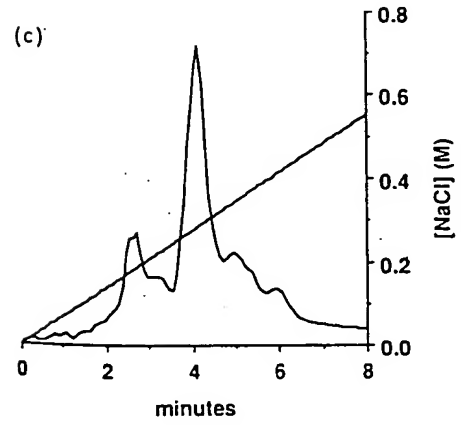

Fig. 20. Scale-up β-galactosidase separation from crude *E. coli* lysate on POROS Q/M; 20 m*M* Tris–HCl buffer, pH 8.0; detection at 280 nm. (a) 100 × 4.6 mm I.D. column; 3.8 mg protein; 4.2 ml/min; 4.8-min gradient to 0.5 *M* NaCl; (b) 100 × 10 mm I.D. column; 18 mg protein; 20 ml/min; 4.8-min gradient to 0.5 *M* NaCl; (c) 100 × 25.4 mm I.D. column; 76 mg protein; 84 ml/min; 7.2-min gradient to 0.5 *M* NaCl.

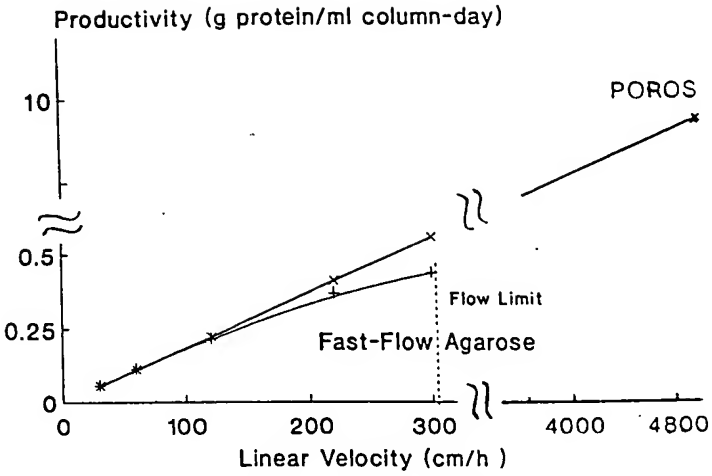

Fig. 21. Column productivity as a function of bed velocity.

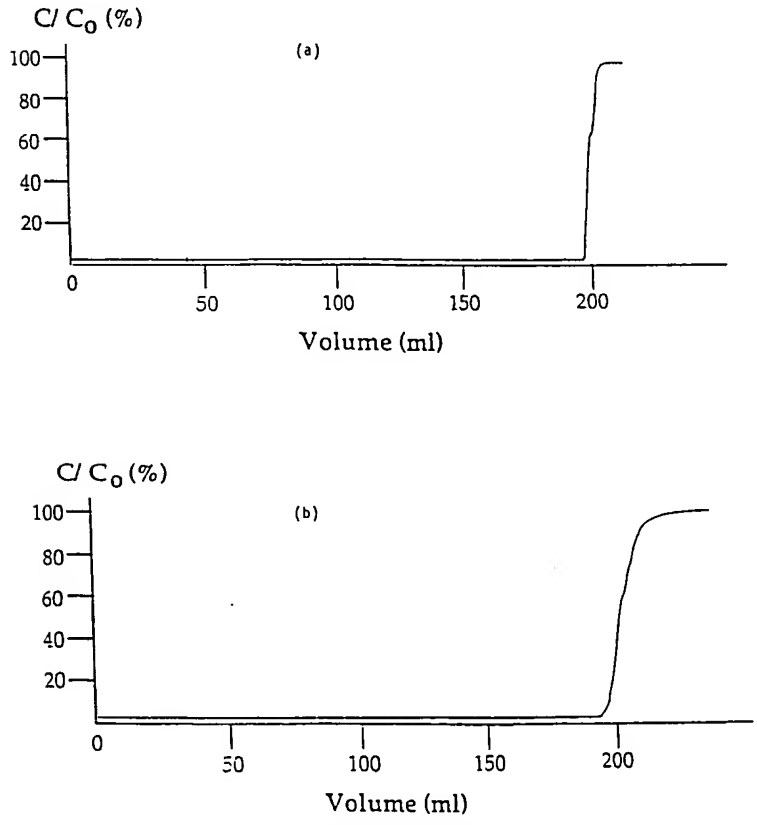

Fig. 22. Solute breakthrough curves for POROS Q/M; 10 mg/ml bovine serum albumin dissolved in 20 m*M* Tris–HCl, pH 8.0; 100 × 25.4 mm I.D. column; detection at 280 nm. (a) 25 ml/min; 300 cm/h; operating pressure, 30 p.s.i.; loading rate, 0.25 g bovine serum albumin/min. (b) 200 ml/min; 2400 cm/h; operating pressure, 350 p.s.i.; loading rate, 2.0 g bovine serum albumin/min.

cm/h is equivalent to that of 300 cm/h operation. However, the loading rate is 2 g bovine serum albumin/min with an operating pressure of 350 p.s.i. (23.3 bar). This number can be compared to the loading rate of an equivalent 50-ml soft gel column, which is about 0.1 g bovine serum albumin/min operating at a linear velocity of 100 cm/h and a negligible backpressure. Packed columns of POROS with a bed height of 1 cm have shown similar capture efficiency as those of 10 cm (data not shown). Therefore, by using columns with a large diameter and short length, these high throughputs should also be possible at backpressures less than 50 p.s.i. (3.3 bar).

CONCLUSIONS

Data presented in this paper show that a chromatographic sorbent with a network of 6000–8000 Å transecting pores interconnected by smaller, 500–1500 Å pores has unique chromatographic properties. First, columns packed with these very-high-porosity materials may be operated at 5–10 times higher mobile phase velocity than conventional 300–1000 Å HPLC packings without loss of resolution. It is concluded that this phenomenon is due to liquid flow through the particles, which convectively transports solute to the active surfaces in the interior of the sorbent. This convective transport is directly coupled to bed mobile phase velocity such that increasing the superficial fluid velocity increases solute flux into the particle and dominates over stagnant phase mass transfer, which is the rate limiting mode of intraparticle transport in conventional porous HPLC media.

Second, the shape of the frontal breakthrough curve, and hence dynamic loading capacity, are virtually independent of mobile phase velocities to 5000 cm/h. This means that there is no significant mass transfer resistance encountered during loading. This too can be due to the perfusion mechanism and also the fact that all of the pores in this sorbent are less than 1 μm in depth. Effectively, the throughpores in the matrix have divided a large particle into an agglomeration of smaller particles that are fed by convective transport.

Finally, it is concluded that the introduction of intraparticle, convective, solute transport is a fundamentally new approach to the reduction of stagnant mobile phase mass transfer limitations in porous materials. This new approach will dramatically decrease separation time and increase throughput and productivity in both analytical and preparative chromatography. Perfusion chromatography combines the high-speed separation ability of convection dominated separation devices (*e.g.* non-porous particles and membranes) with the high capacity of porous HPLC supports while operating at medium to low pressures.

SYMBOLS

$(dp/dx)_c$	pressure gradient across the column
a, b, c, c'	constants in Van Deemter equation
A_c	column cross-sectional area
C	solute concentration in column effluent
C_0	initial solute concentration
D	solute diffusion coefficient in the pores
D_{eff}	modified solute diffusivity

lved in 20 m*M*
m/h; operating
m/h; operating

d_p	particle diameter
d_m	microsphere diameter
d_{pore}	particle throughpore diameter
F	mobile phase volumetric flow-rate
H	plate height equivalent to a theoretical plate
h	reduced plate height
K	packed column permeability
K_L	equilibrium constant
K_p	particle permeability
L	column length
M	overall dimensionless mass transfer coefficient
M_{pore}	dimensionless pore mass transfer coefficient
N	Number of theoretical plates/column
Pe	Peclet number
Q_{max}	equilibrium saturation capacity
r	constant relating microsphere diameter to throughpore diameter
R_s	resolution
t	time
u_{bed}	column superficial fluid velocity (F/A_c)
u_{pore}	velocity in a throughpore
V_t	elution volume
W	peak width at half peak height
ε_b	packed column void fraction
ε_p	particle void fraction
η	mobile phase viscosity
κ	constant relating pore velocity to superficial fluid velocity

ACKNOWLEDGEMENTS

The authors gratefully acknowledge Rolf Jansen for his technical assistance. The authors also wish to acknowledge the assistance of Dr. Charles Bracker and his laboratory, the Purdue Agricultural Experiment Station Electron Microscopy Center, for carrying out the SEM studies. The technical assistance of Mary Anne Rounds is acknowledged.

REFERENCES

1 E. A. Peterson and H. A. Sober, *J. Am. Chem. Soc.*, 78 (1956) 751.
2 J. Porath and P. Flodin, *Nature (London)*, 183 (1959) 1657.
3 S. H. Chang, K. M. Gooding and F. E. Regnier, *J. Chromatogr.*, 125 (1976) 103.
4 L. Fagerstam, L. Soderberg, L. Waahlstrom, U.-B. Fredriksson, K. Plith and E. Wallden, *Protides Biol. Fluids*, 30 (1982) 621.
5 J. C. Giddings, *Dynamics of Chromatography, Part I, Principles and Theory*, Marcel Dekker, New York, 1965.
6 Cs. Horváth and H.-J. Lin, *J. Chromatogr.*, 149 (1978) 43.
7 J. F. K. Huber, *Ber. Bunsenges. Phys. Chem.*, 77 (1973) 179.
8 L. R. Synder and J. J. Kirkland, *Introduction to Modern Liquid Chromatography*, Wiley, New York, 2nd ed., 1979.
9 A. J. P. Martin and R. L. M. Synge, *Biochem. J.*, 35 (1941) 1358.

10 R. E. Majors, *Anal. Chem.*, 44 (1972) 1722.
11 K. K. Unger, R. Kern, M. C. Ninov and K.-F. Krebs, *J. Chromatogr.*, 99 (1974) 435.
12 K. K. Unger, G. Jilge, J. N. Kinkel and M. T. W. Hearn, *J. Chromatogr.*, 359 (1986) 61.
13 K. Kalghatgi and Cs. Horváth, *J. Chromatogr.*, 398 (1987) 335.
14 K. Kalghatgi and Cs. Horváth, *J. Chromatogr.*, 443 (1988) 343.
15 S. J. Gibbs and E. N. Lightfoot, *I&EC Fundam.*, 490 (1986) 25.
16 C. M. Guttman and E. A. DiMarzio, *Macromolecules*, 3 (1970) 681.
17 M. E. van Kreveld and N. van den Hoed, *J. Chromatogr.*, 149 (1978) 71.
18 O. Chiantore and M. Guaita, *J. Liq. Chromatogr.*, 5 (1982) 643.
19 W. Haller, *U.S. Pat.*, 3 549 524 (1971).
20 J. Lieto, D. Milstein, R. L. Albright, J. V. Minkiewicz and B. C. Gates, *Chemtech*, January (1983) 46.
21 R. E. Kesting, *Synthetic Polymeric Membranes*, New York, 2nd ed., 1985.
22 W. Kopaciewicz, M. A. Rounds and F. E. Regnier, *J. Chromatogr.*, 362 (1986) 187.
23 N. B. Afeyan, R. C. Dean and F. E. Regnier, *U.S. Pat. Appl.*, 376 885 (1989).
24 R. B. Bird, W. E. Stewart and E. N. Lightfoot, *Transport Phenomena*, Wiley, New York, 1960.
25 W. M. Deen, *AIChE J.*, 1409, 33 (1987).
26 J. J. van Deemter, F. J. Zuiderweg and A. Klinkenberg, *Chem. Eng. Sci.*, 5 (1956) 271.
27 N. K. Hiester and T. Vermeulen, *Chem. Eng. Prog.*, 48 (1952) 505.
28 F. H. Arnold, H. W. Blanch and C. R. Wilke, *Chem. Eng. J.*, 30 (1985) B9.
29 W. Kopaciewicz and S. P. Fulton and S. Y. Lee, *J. Chromatogr.*, 409 (1988) 111.
30 H. A. Chase, *J. Chromatogr.*, 297 (1984) 179.
31 K. Buchholz, *Biotech. Lett.*, 1 (1979) 451.
32 S. W. Carleysmith, M. B. L. Eames and M. D. Lilly, *Biotechnol. Bioeng.*, 22 (1980) 957.
33 D. D. Do, *Biotechnol. Bioeng.*, 26 (1984) 1032.
34 N. B. Afeyan, N. F. Gordon and C. L. Cooney, *J. Chromatogr.*, 478 (1989) 1.
35 N. F. Gordon, *Ph.D. Thesis*, MIT, Cambridge, MA, 1989.
36 G. L. Skidmore and H. A. Chase, in *Ion Exchange for Industry*, Ellis Horwood, Chichester, 1988, p. 520.